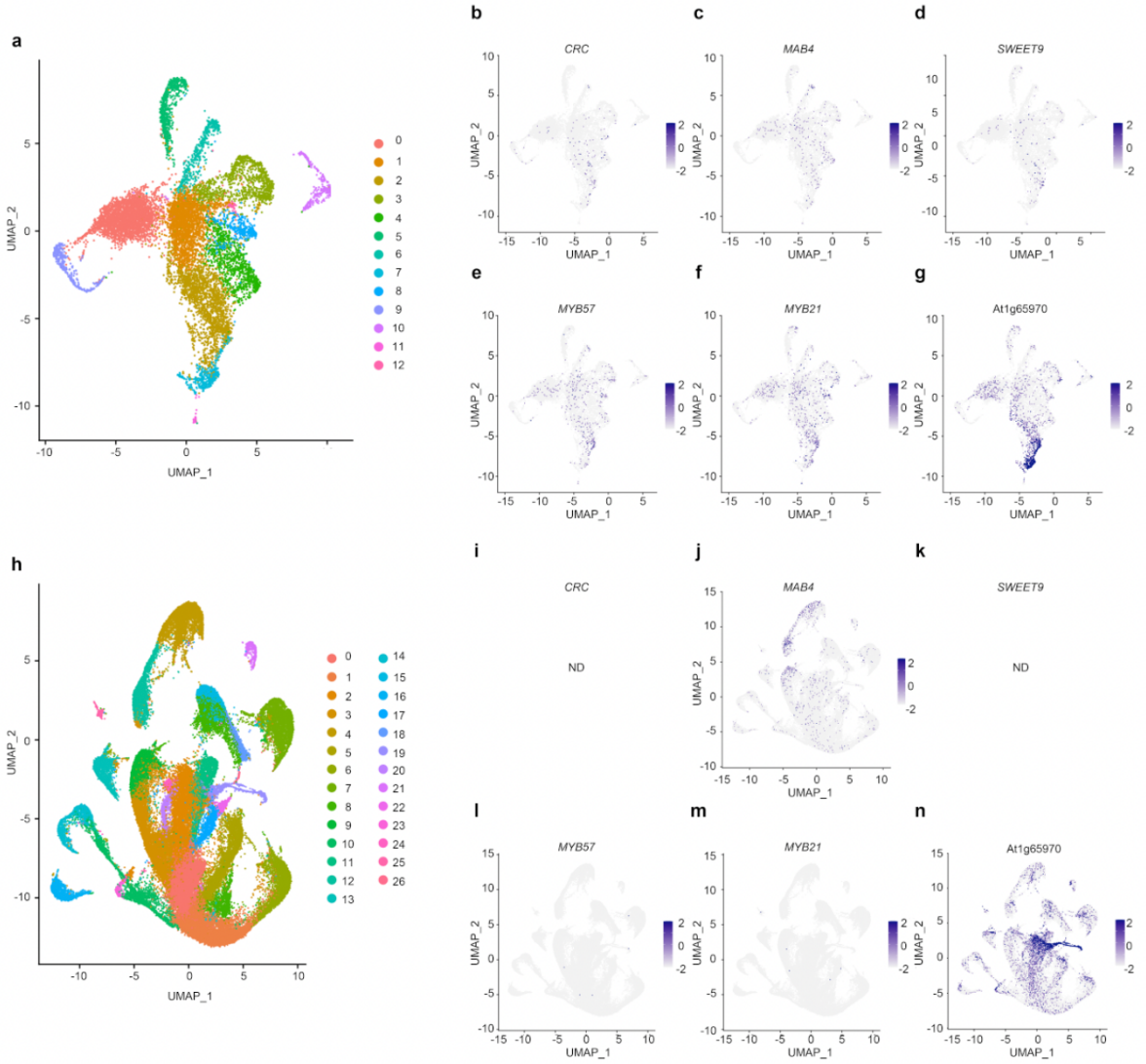

Supplementary Fig. 1 Single-nucleus RNA-seq (scRNA-seq) analysis of flowers and siliques in *Arabidopsis thaliana.*
a, Clustering of snRNA-seq profiles using the flower dataset. A Uniform Manifold Approximation and Projection (UMAP) plot of all individual cells (dots) is shown, with the 12 clusters identified using Seurat color-coded. **b–g**, Expression of literature-based nectary marker genes in the flower snRNA-seq dataset: *CRC* (**b**), *MAB4* (**c**), *SWEET9* (**d**), *MYB57* (**e**), *MYB21* (**f**), and At1g65970 (**g**). **h,** Clustering of snRNA-seq profiles using the silique dataset. A UMAP plot is shown, with the 26 clusters identified using Seurat color-coded. **I–n**, Expression of literature-based nectary marker genes in the silique dataset: *CRC* (**i**), *MAB4* (**j**), *SWEET9* (**k**), *MYB57* (**l**), *MYB21* (**m**) and At1g65970 (**n**).

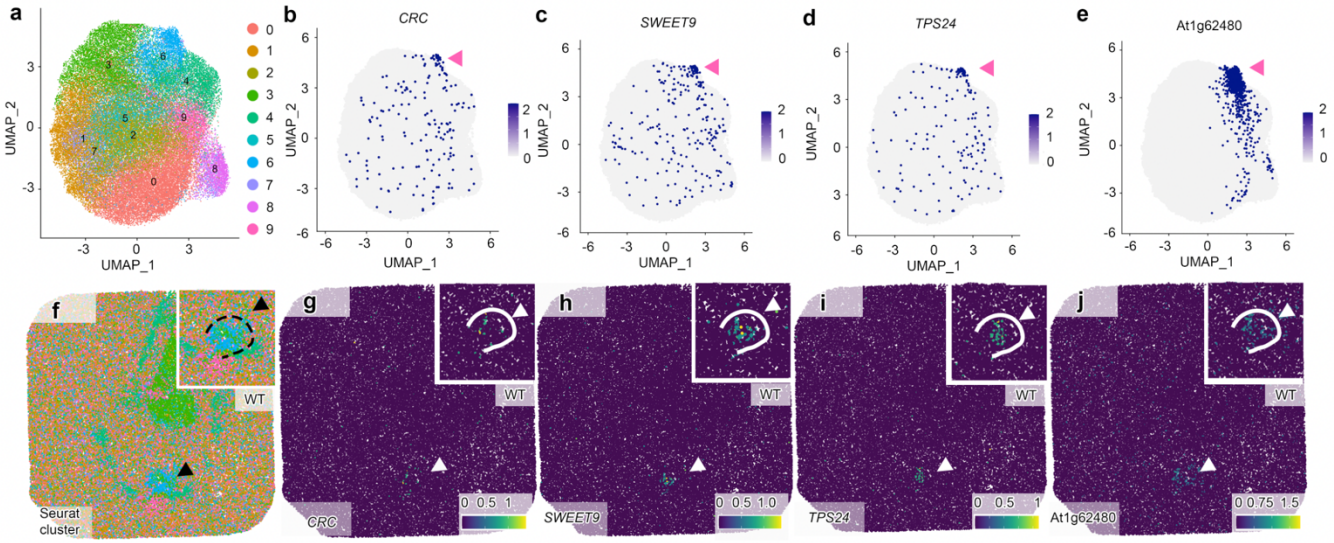

Supplementary Fig. 2 Slide-seq replicates in wild-type nectaries.

a, UMAP plot of the Curio Seeker spot transcriptome cluster from nectary sections in wild type. Seurat clusters are color-coded into 10 colors using Seurat's default color palette. **b–e**, Expression of nectary-specific genes on the UMAP plot of Slide-seq data in wild type: *CRC* (**b**), *SWEET9* (**c**), *TPS24* (**d**), and At1g62480 (**e**). The position of cluster 6 is indicated by the pink arrowheads. **f,** Spatial map of Seurat clusters by Slide-seq in a wild-type nectary. Black arrowheads indicate the location of the nectary, with the dashed line outlining its shape. **g–j**, Spatial map of nectary-specific genes by Slide-seq in wild type: *CRC* (**g**), *SWEET9* (**h**), *TPS24* (**i**) and At1g62480 (**j**). White arrowheads indicate the location of the nectary, while the solid lines outline its shape.

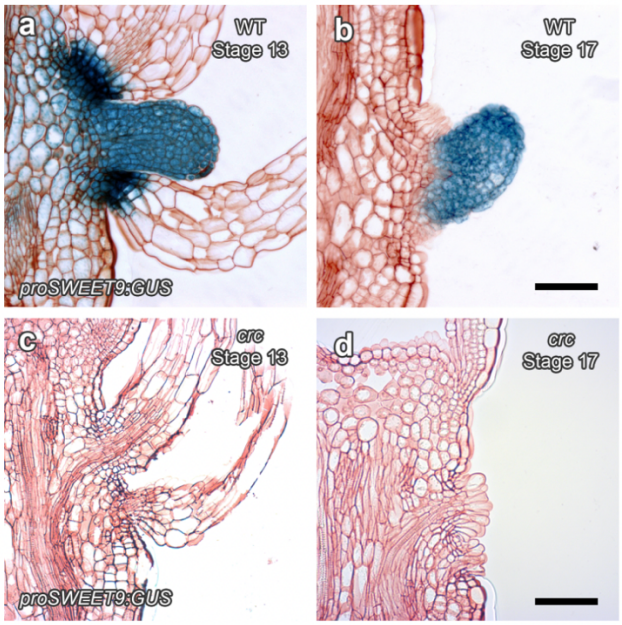

Supplementary Fig. 3 GUS staining from the *proSWEET9:GUS* reporter in wild type and *crc*.
GUS activity in longitudinal sections of nectary from stage 13 (**a, c**) or stage 17 (**b, d)** flowers from wild type (**a, b**) or the *crc* mutant (**c, d**) harboring the *proSWEET9:GUS* reporter. Scale bars, 50 µm.

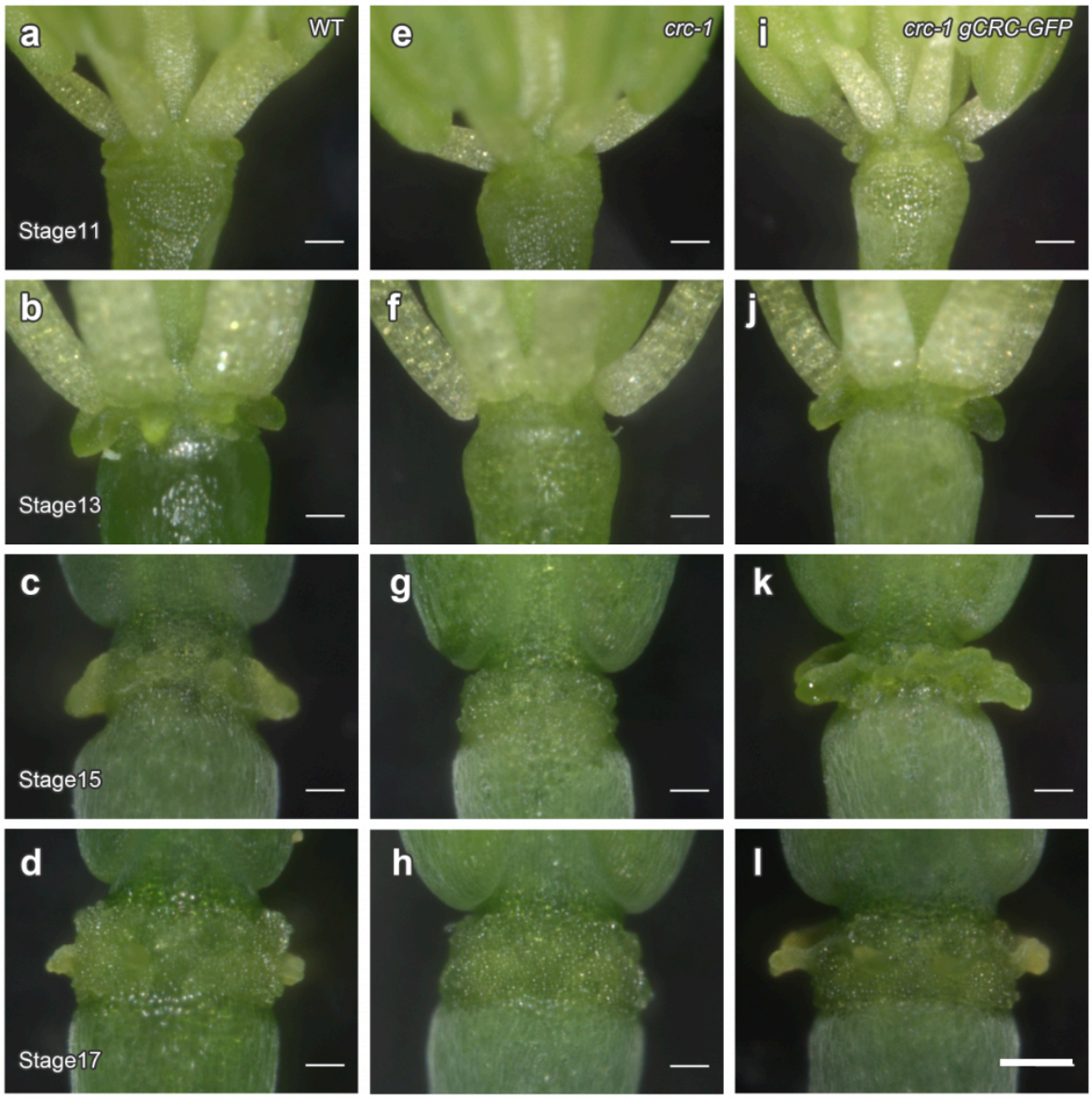

Supplementary Fig. 4 Close-up views of nectaries from the flowers of *crc-1 gCRC-GFP* plants.
a–d, Side views of nectaries from wild-type (WT, L*er*) flowers at stage 11 (**a**), stage 13 (**b**), stage 15 (**c**) and stage 17 (**d**). **e–h**, Side views of nectaries from *crc-1* flowers at stage 11 (**e**), stage 13 (**f**), stage 15 (**g**) and stage 17 (**h**). **i–l**, Side views of nectaries from *crc-1 gCRC-GFP* flowers at stage 11 (**i**), stage 13 (**j**), stage 15 (**k**) and stage 17 (**l**). Scale bars, 200 μm.

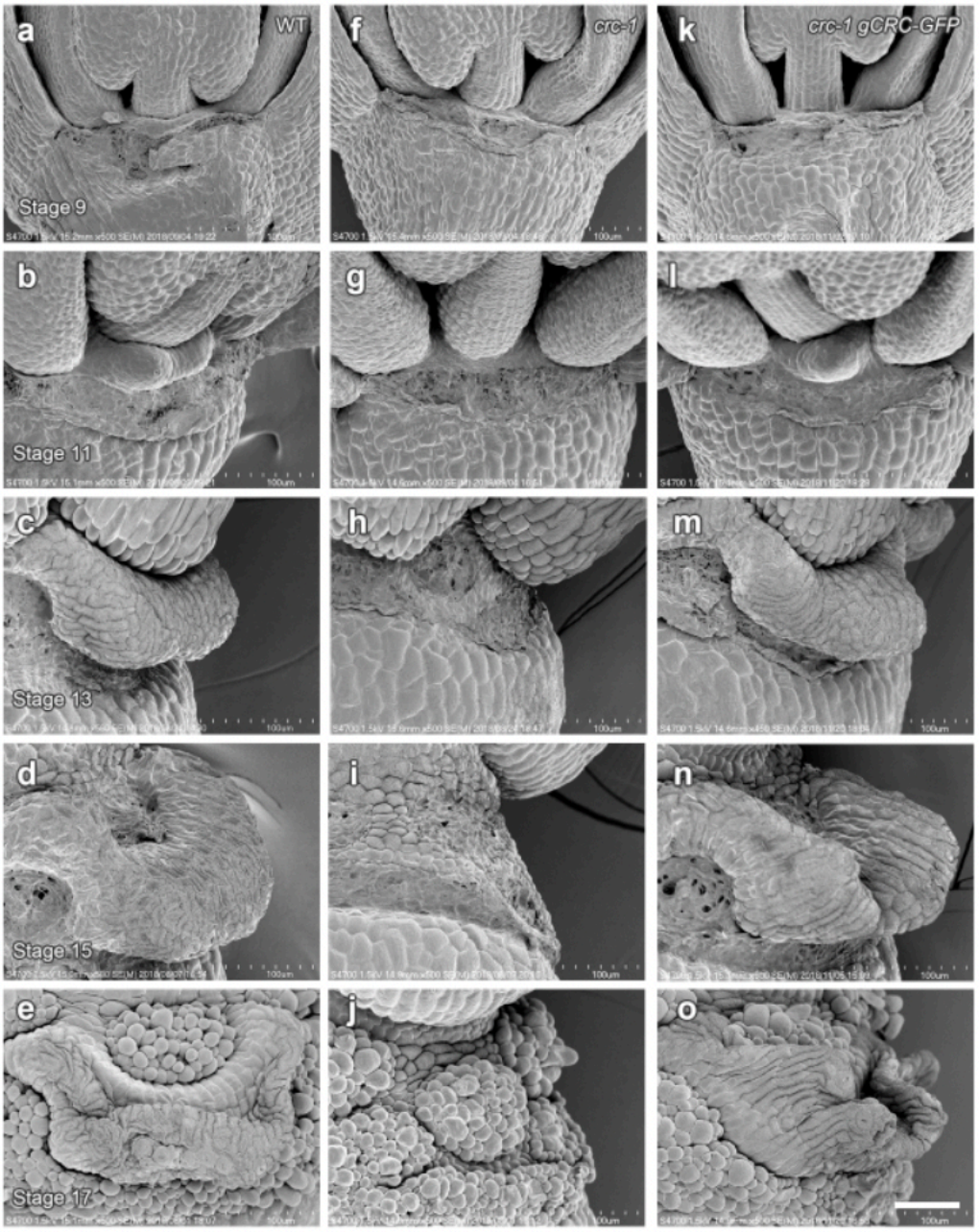

Supplementary Fig. 5 Surface structure of nectaries from *crc-1 gCRC-GFP* flowers. **a–e**, SEM images of nectaries from WT (L*er*) flowers at stage 9 (**a**), stage 11 (**b**), stage 13 (**c**), stage 15 (**d**) and stage 17 (**e**). **f–j**, SEM images of nectaries from *crc-1* flowers at stage 9 (**f**), stage 11 (**g**), stage 13 (**h**), stage 15 (**i**) and stage 17 (**j**). **k–o**, SEM images of nectaries from *crc-1 gCRC-GFP* flowers at stage 9 (**k**), stage 11 (**l**), stage 13 (**m**), stage 15 (**n**) and stage 17 (**o**). Scale bar, 50 μm.

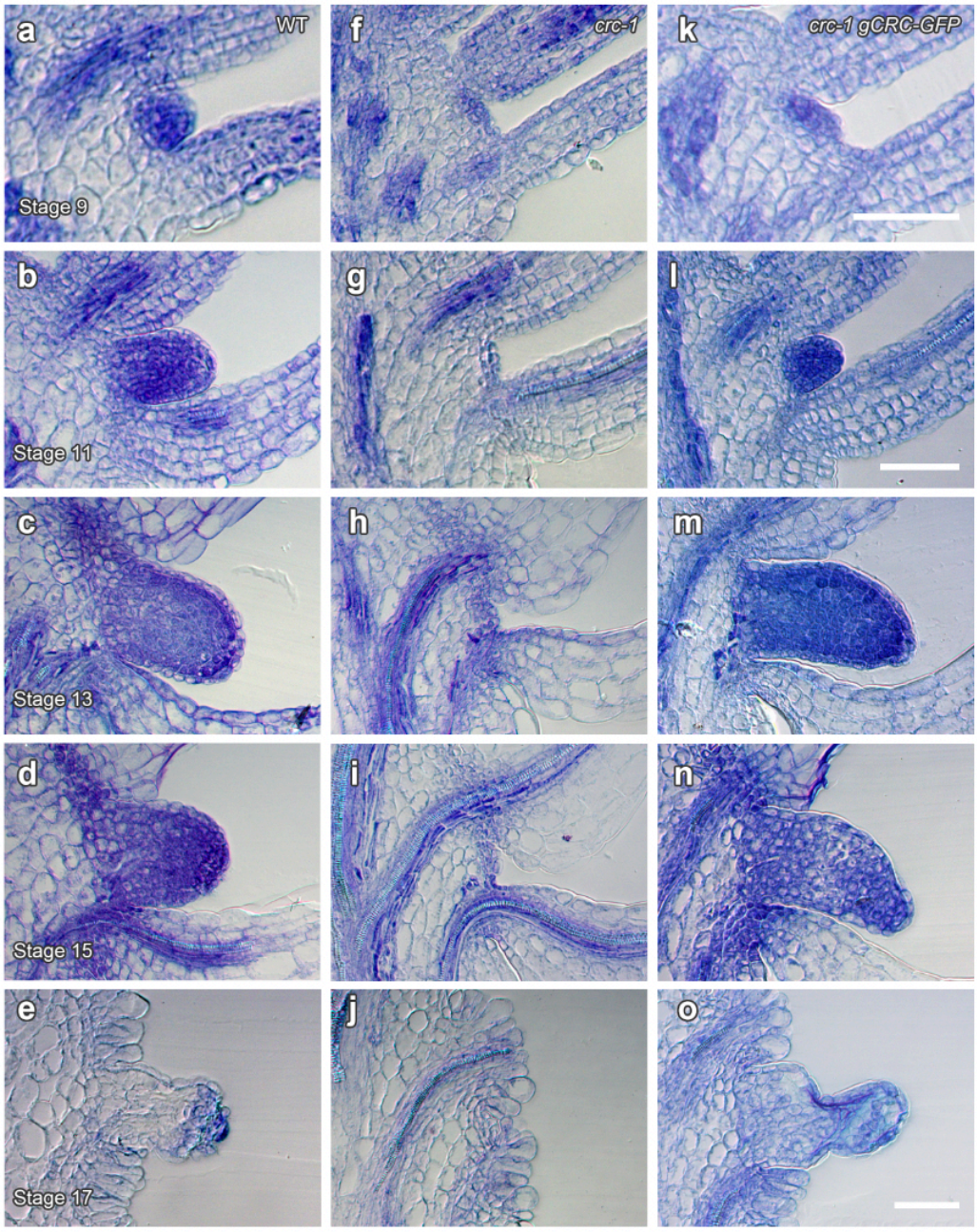

Supplementary Fig. 6 Internal structure of nectaries from *crc-1 gCRC-GFP* flowers. **a–e**, Longitudinal sections of nectaries from WT (L*er*) flowers at stage 9 (**a**), stage 11 (**b**), stage 13 (**c**), stage 15 (**d**) and stage 17 (**e**). **f–j**, Longitudinal sections of nectaries from *crc-1* flowers at stage 9 (**f**), stage 11 (**g**), stage 13 (**h**), stage 15 (**i**) and stage 17 (**j**). **k–o**, Longitudinal sections of nectaries from *crc-1 gCRC-GFP* flowers at stage 9 (**k**), stage 11 (**l**), stage 13 (**m**), stage 15 (**n**) and stage 17 (**o**). Scale bars, 50 μm.

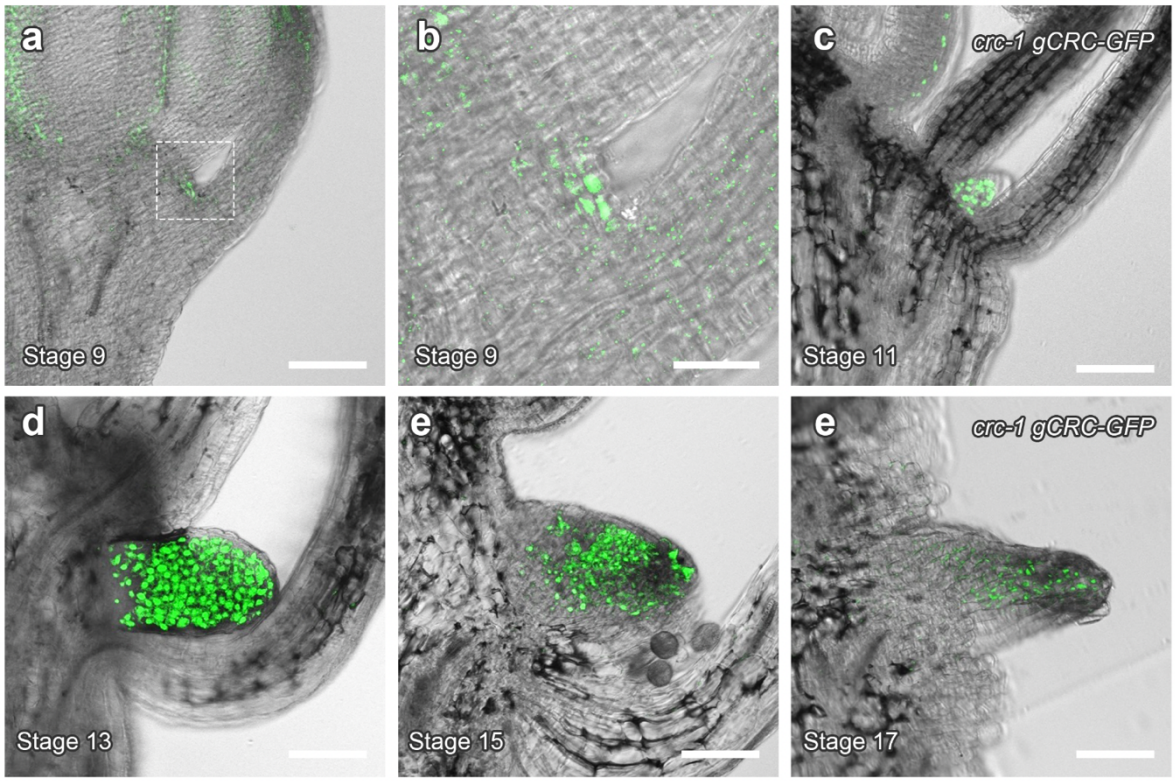

Supplementary Fig. 7 Pattern of GFP fluorescence in nectaries from *crc-1 gCRC-GFP* flowers.
a–f, GFP fluorescence in longitudinal sections of nectaries from *crc-1 gCRC-GFP* flowers at stage 9 (**a, b**), stage 11 (**c**), stage 13 (**d**), stage 15 (**e**) and stage 17 (**f**). Panel (**b**) is an enlarged view of panel (**a**). Scale bars, 50 μm (a, c-e), 10 μm (b).

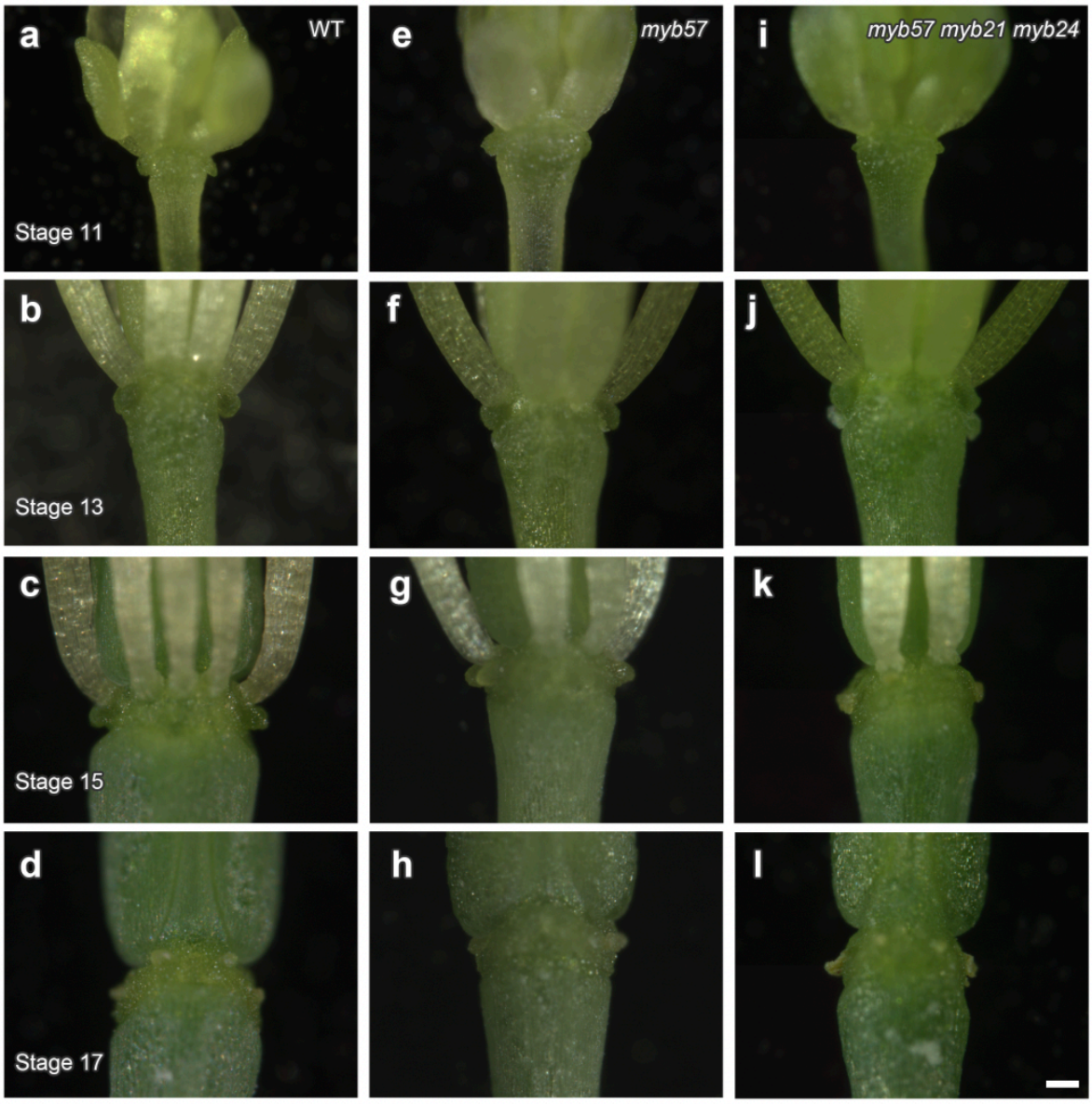

Supplementary Fig. 8 Close-up views of nectaries from *myb* mutant flowers. **a–d**, Side views of nectaries from WT (Col-0) flowers at stage 11 (**a**), stage 13 (**b**), stage 15 (**c**) and stage 17 (**d**). **e–h**, Side views of nectaries from *myb57-2* flowers at stage 11 (**e**), stage 13 (**f**), stage 15 (**g**) and stage 17 (**h**). **i–l**, Side views of nectaries from *myb57-2 myb21-1 myb24-1* flowers at stage 11 (**i**), stage 13 (**j**), stage 15 (**k**) and stage 17 (**l**). Scale bar, 100 μm.

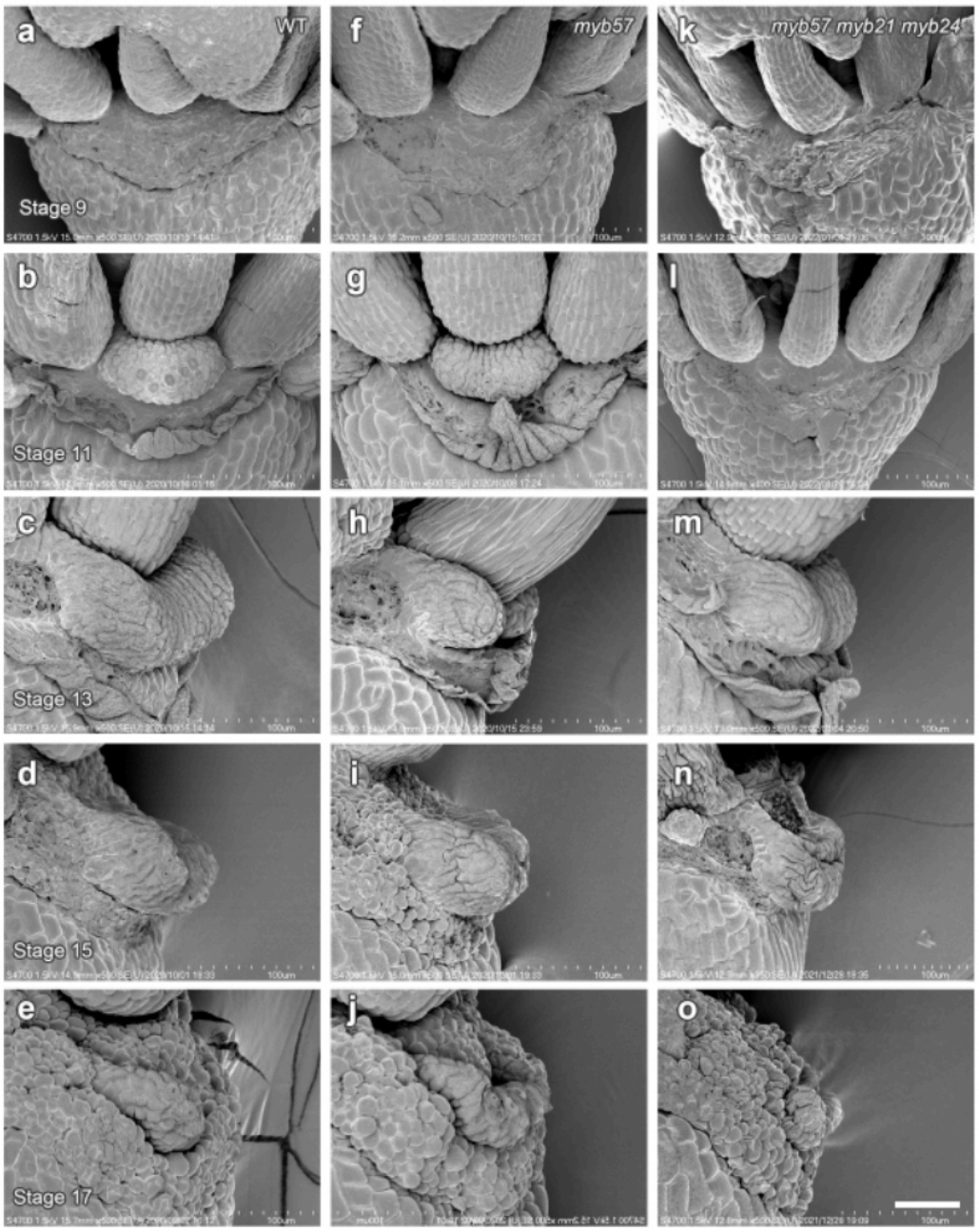

Supplementary Fig. 9 Surface structure of a nectary from *myb* mutant flowers. **a–e**, SEM images of nectaries from WT (Col-0) flowers at stage 9 (**a**), stage 11 (**b**), stage 13 (**c**), stage 15 (**d**) and stage 17 (**e**). **f–j**, SEM images of nectaries from *myb57-2* flowers at stage 9 (**f**), stage 11 (**g**), stage 13 (**h**), stage 15 (**i**) and stage 17 (**j**). **k–o**, SEM images of nectaries from *myb57-2 myb21-1 myb24-1* flowers at stage 9 (**k**), stage 11 (**l**), stage 13 (**m**), stage 15 (**n**) and stage 17 (**o**). Scale bar, 50 μm.

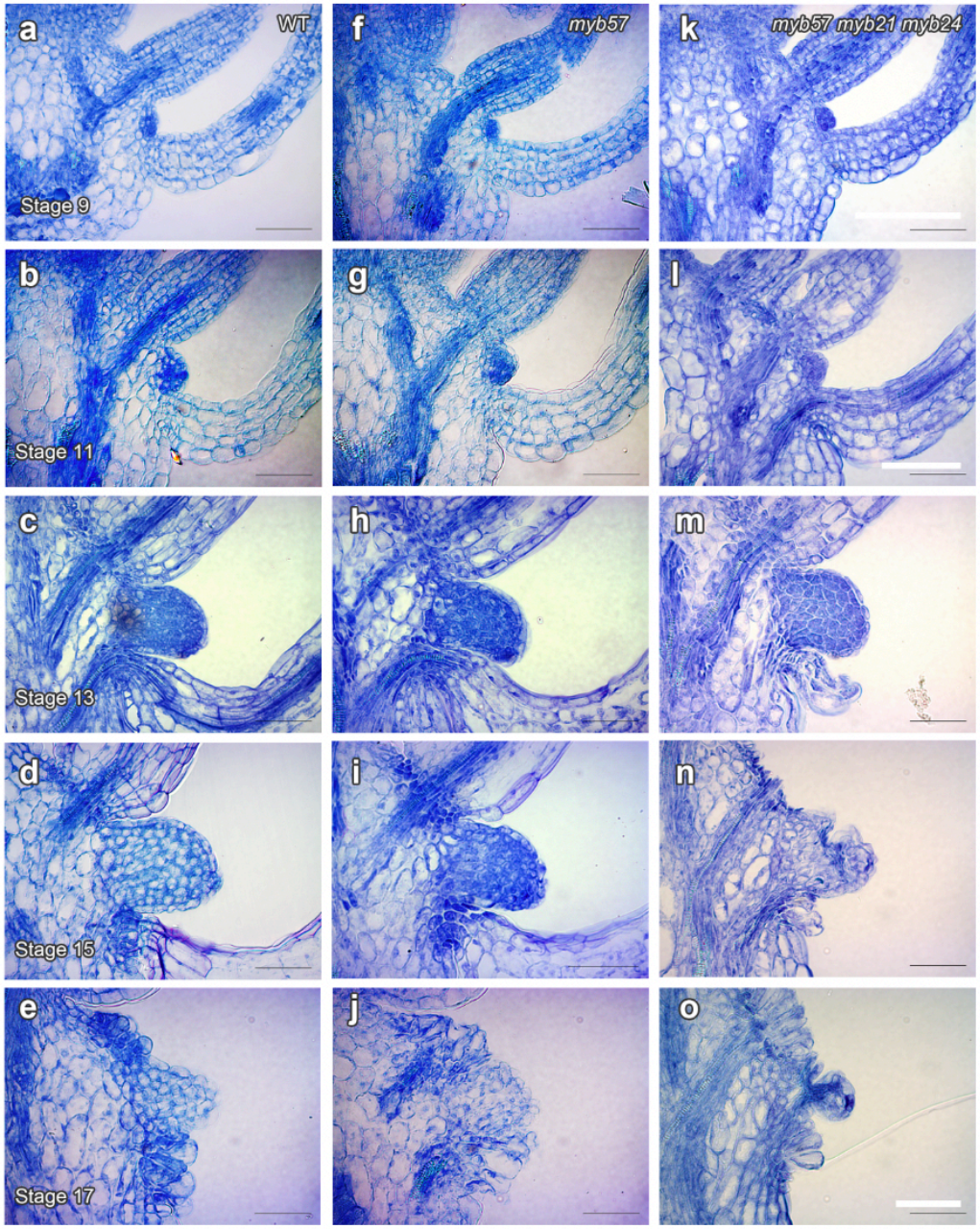

Supplementary Fig. 10 Internal structure of a nectary from *myb* mutant flowers. **a–e**, Longitudinal sections of nectaries from WT (Col-0) flowers at stage 9 (**a**), stage 11 (**b**), stage 13 (**c**), stage 15 (**d**) and stage 17 (**e**). **f–j**, Longitudinal sections of nectaries from *myb57-2* flowers at stage 9 (**f**), stage 11 (**g**), stage 13 (**h**), stage 15 (**i**) and stage 17 (**j**). **k–o**, Longitudinal sections of nectaries from *myb57-2 myb21-1 myb24-1* flowers at stage 9 (**k**), stage 11 (**l**), stage 13 (**m**), stage 15 (**n**) and stage 17 (**o**). Scale bars, 50 μm.

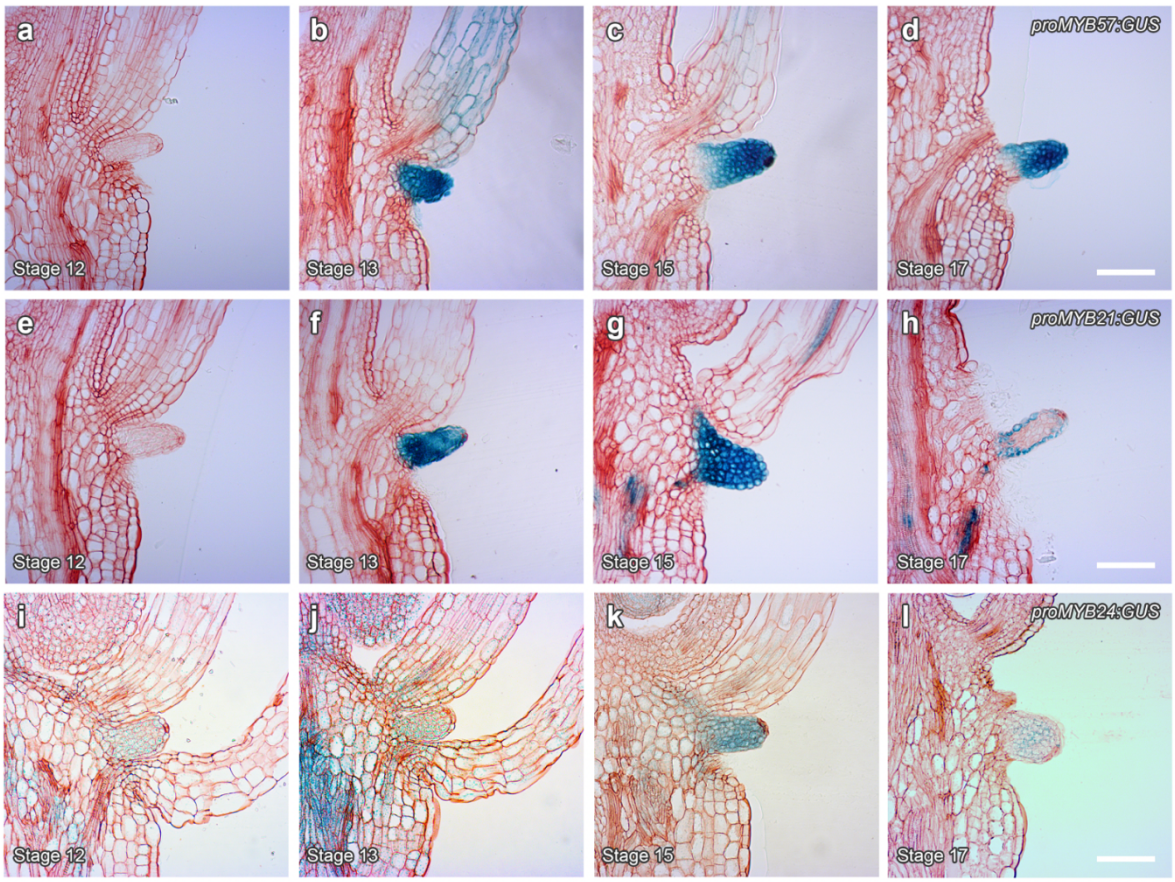

Supplementary Fig. 11 Expression of *MYB* family genes in a nectary. **a–d**, GUS activity in longitudinal sections from a nectary of a WT (Col-0) flower harboring the *proMYB57:GUS* reporter at stage 12 (**a**), stage 13 (**b**), stage 15 (**c**) and stage 17 (**d**). **e–h**, GUS activity in longitudinal sections from a nectary of a WT flower carrying the *proMYB21:GUS* reporter at stage 12 (**e**), stage 13 (**f**), stage 15 (**g**) and stage 17 (**h**). **i–l**, GUS activity in longitudinal sections from a nectary of a WT flower harboring the *proMYB24:GUS* reporter at stage 12 (**i**), stage 13 (**j**), stage 15 (**k**) and stage 17 (**l**). Scale bars, 50 μm.

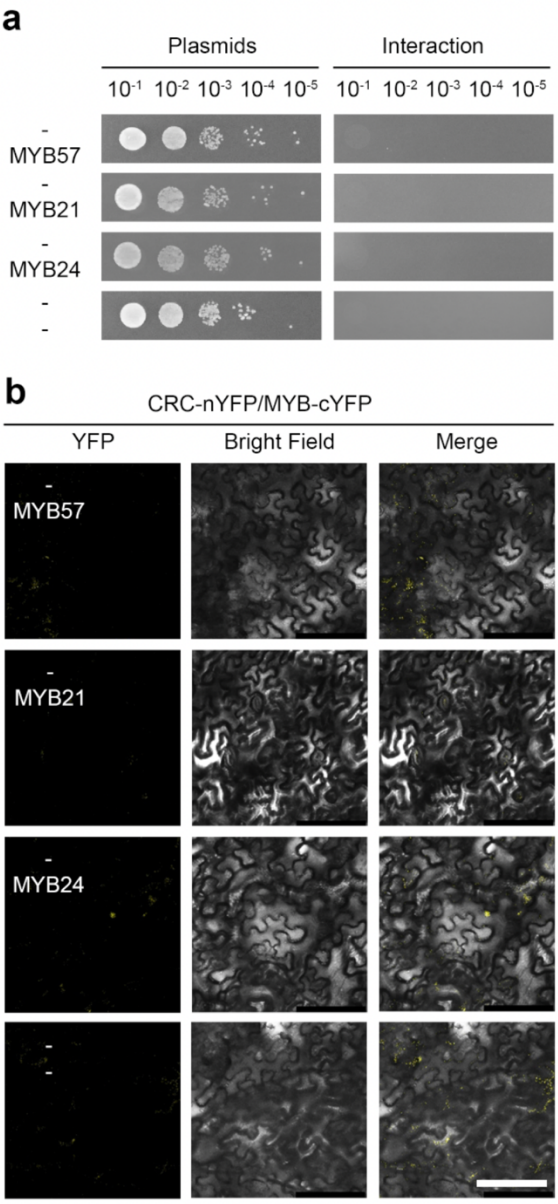

Supplementary Fig. 12 Controls for the physical interaction between CRC and MYBs.
a, Negative control of the yeast two-hybrid assay on synthetic defined (SD) medium lacking tryptophan and leucine (left; control medium) and SD medium lacking tryptophan, leucine and histidine (right; selection medium). Ten-fold serial dilutions of each positive yeast colony were spotted. **b**, Negative control for the BiFC assay in *N. benthamiana*. Left, YFP fluorescence; middle, bright-field image; right, merge. Scale bar, 50 μm.

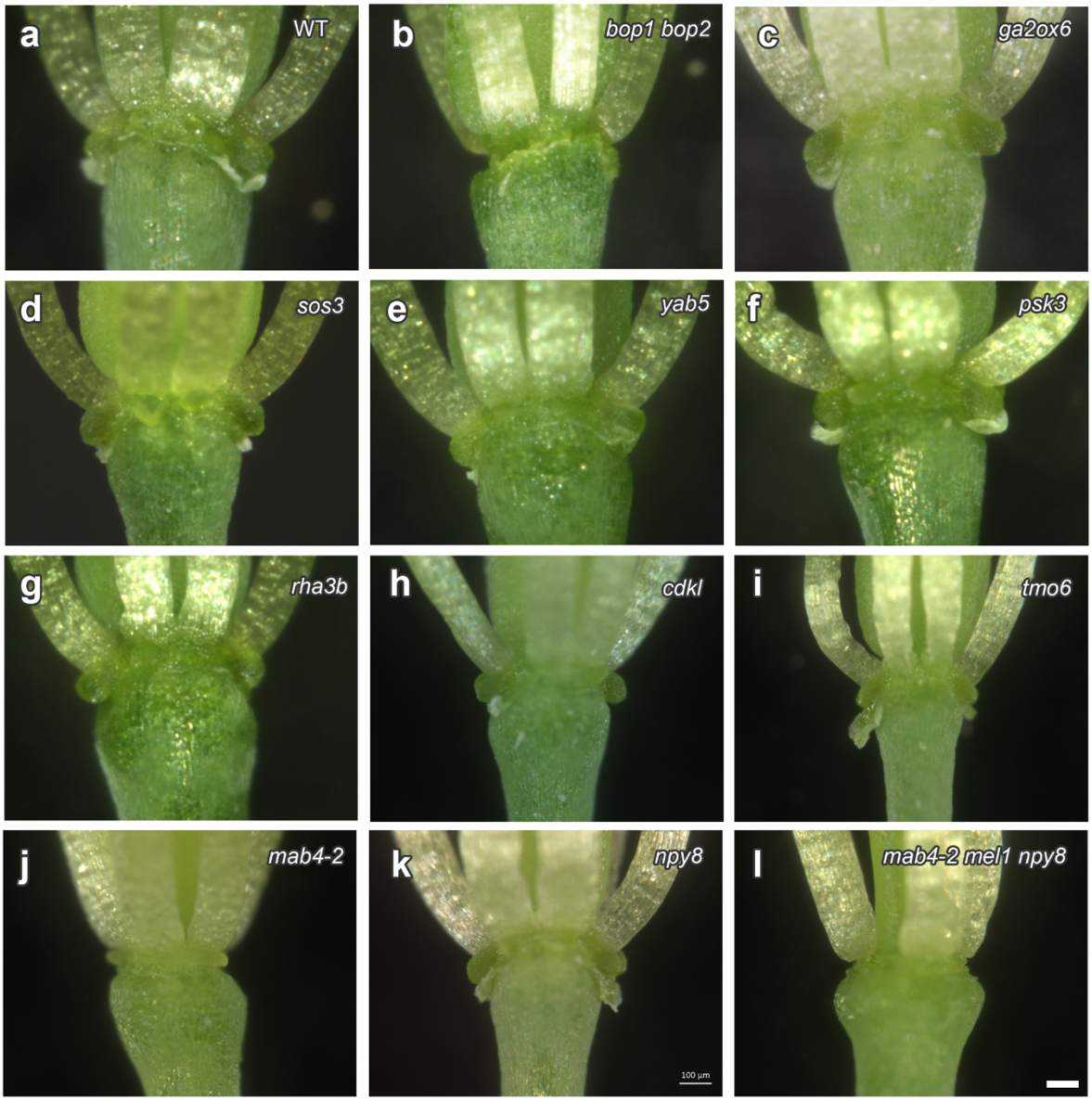

Supplementary Fig. 13 Close-up views of nectaries in the flowers of various mutants.
a–l, Side views of nectaries from stage 13 flowers of WT (Col-0) (**a**), *bop1 bop2* (**b**), *ga2ox6* (**c**), *sos3* (**d**), *yab5* (**e**), *psk3* (**f**), *rha3b* (**g**), *cdkl* (**h**), *tmo6* (**i**), *mab4-2* (**j**), *npy8* (**k**) and *mab4-2 mel1 npy8* (**l**) plants. Scale bar, 100 µm.

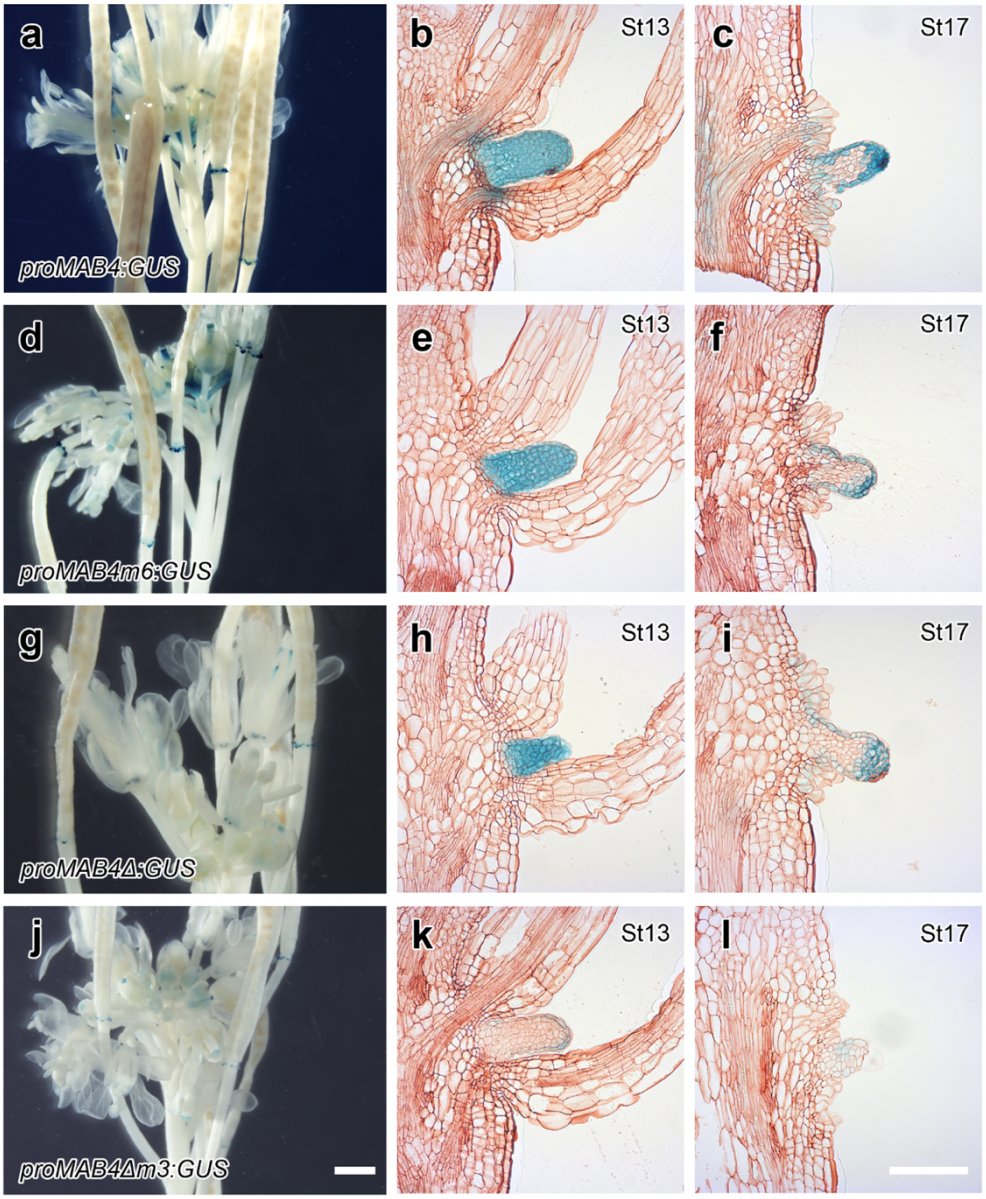

Supplementary Fig. 14 Detection of transcriptional activity from the intact or mutated *MAB4* promoter.
a, d, g, j, GUS activity from inflorescences of *proMAB4:GUS* (**a**), *proMAB4m6:GUS* (**d**), *proMAB4Δ:GUS* (**g**) and *proMAB4*Δm3*:GUS* (**j**) plants. Scale bars, 1 mm. **b, e, h, k**, Longitudinal sections of a nectary from a *proMAB4:GUS* (**b**), *proMAB4m6:GUS* (**e**), *proMAB4Δ:GUS* (**h**) and *proMAB4*Δm3*:GUS* (**k**) plant at stage 13. **c, f, i, l,** Longitudinal sections of a nectary from a *proMAB4:GUS* (**c**), *proMAB4m6:GUS* (**f**), *proMAB4Δ:GUS* (**i**) and *proMAB4*Δm3*:GUS* (**l**) plant at stage 17. Scale bars, 100 µm. The transgenic line with the average GUS activity level for each transgene is shown.

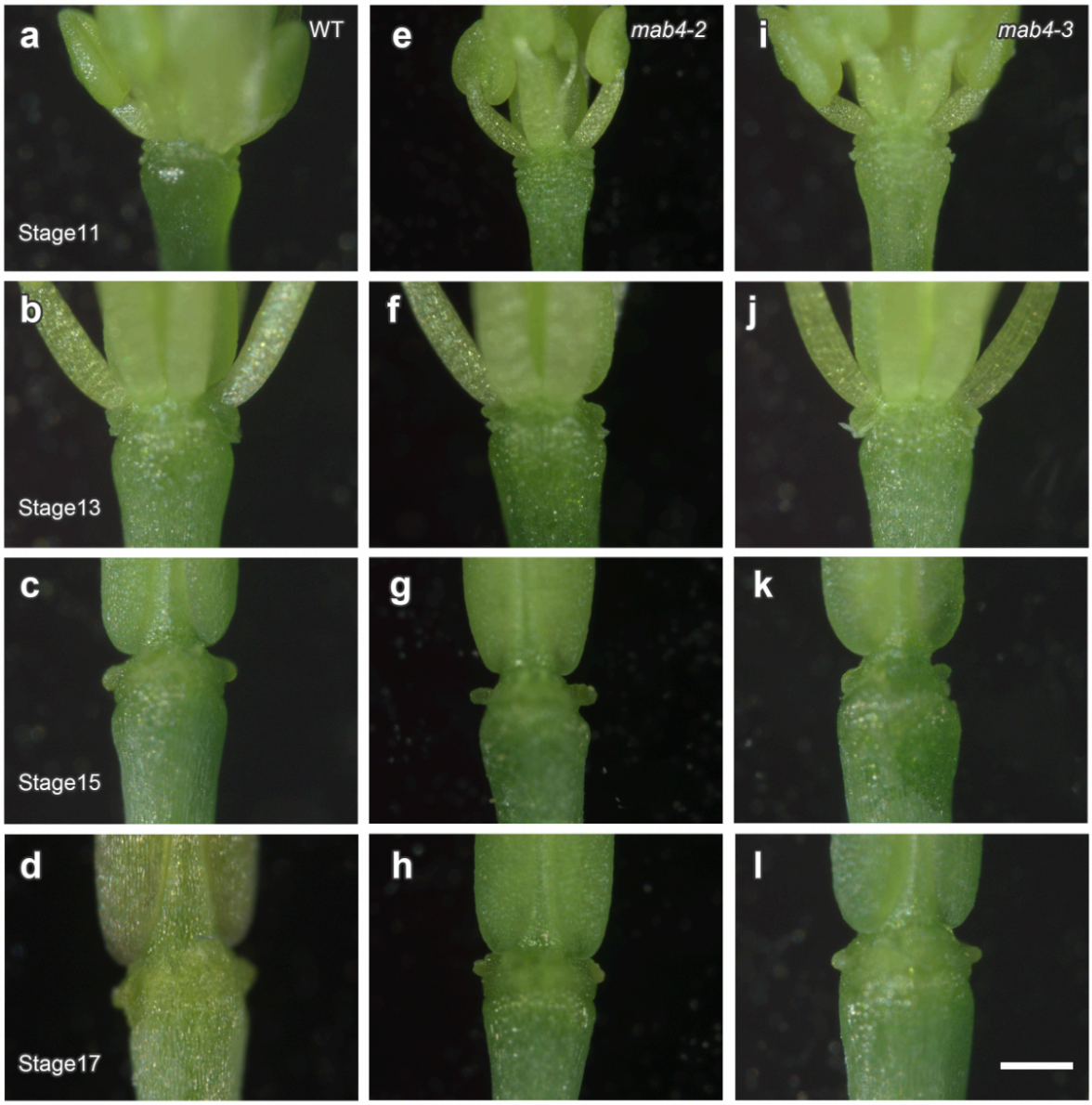

Supplementary Fig. 15 Close-up views of nectaries in the flowers of *mab4* mutants. **a–d**, Side views of nectaries from WT (Col-0) flowers at stage 11 (**a**), stage 13 (**b**), stage 15 (**c**) and stage 17 (**d**). **e–h**, Side views of nectaries from *mab4-2* flowers at stage 11 (**e**), stage 13 (**f**), stage 15 (**g**) and stage 17 (**h**). **i–l**, Side views of nectaries from *mab4-3* flowers at stage 11 (**i**), stage 13 (**j**), stage 15 (**k**) and stage 17 (**l**). Scale bar, 200 μm.

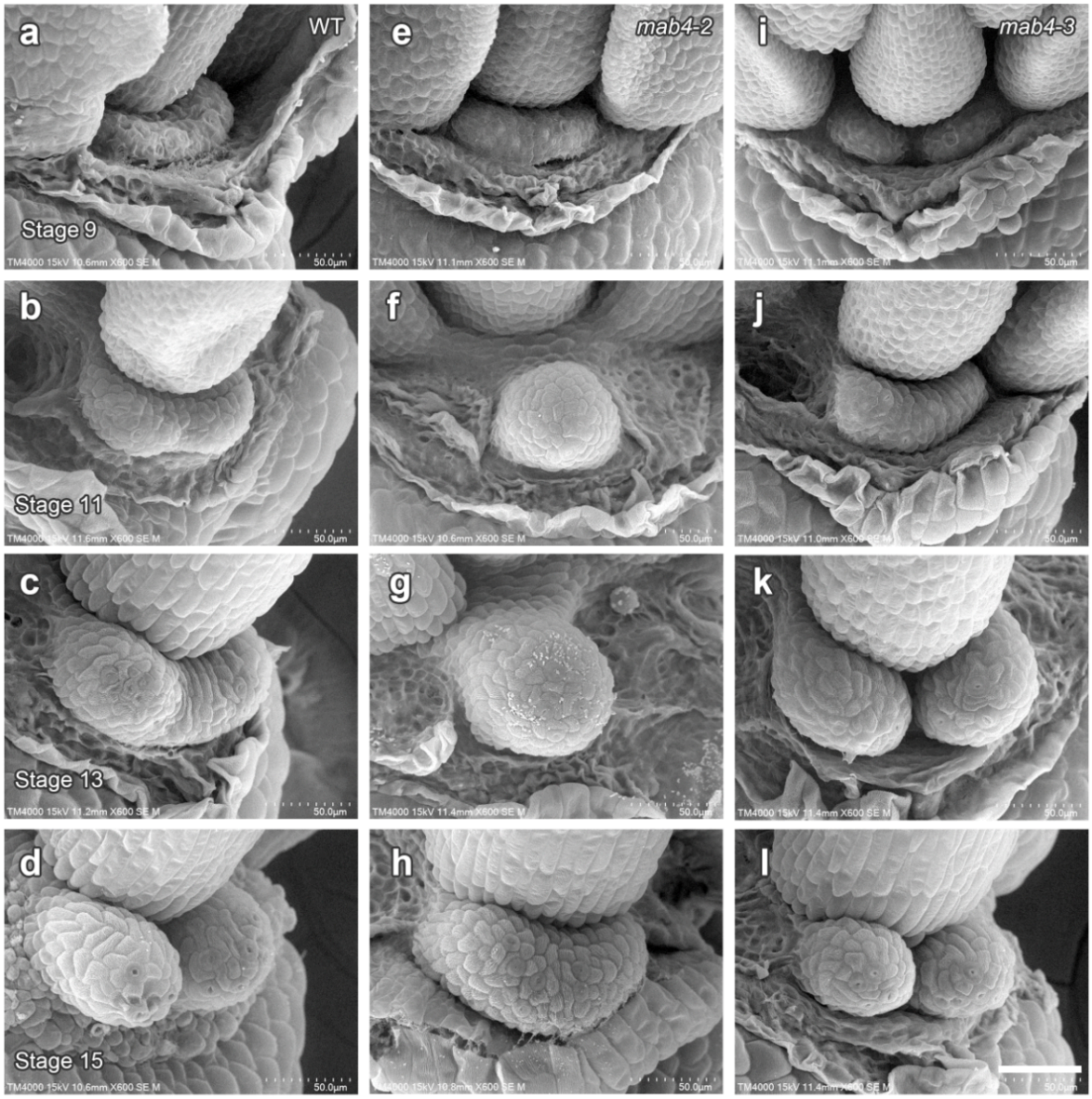

Supplementary Fig. 16 Surface structure of nectaries in the flowers of *mab4* mutants.
a–d, SEM images of nectaries from WT (Col-0) flowers at stage 9 (**a**), stage 11 (**b**), stage 13 (**c**), and stage 15 (**d**). **e–h**, SEM images of nectaries from *mab4-2* flowers at stage 9 (**e**), stage 11 (**f**), stage 13 (**g**), and stage 15 (**h**). **i–l**, SEM images of nectaries from *mab4-3* flowers at stage 9 (**i**), stage 11 (**j**), stage 13 (**k**), and stage 15 (**l**). Scale bar, 50 μm.

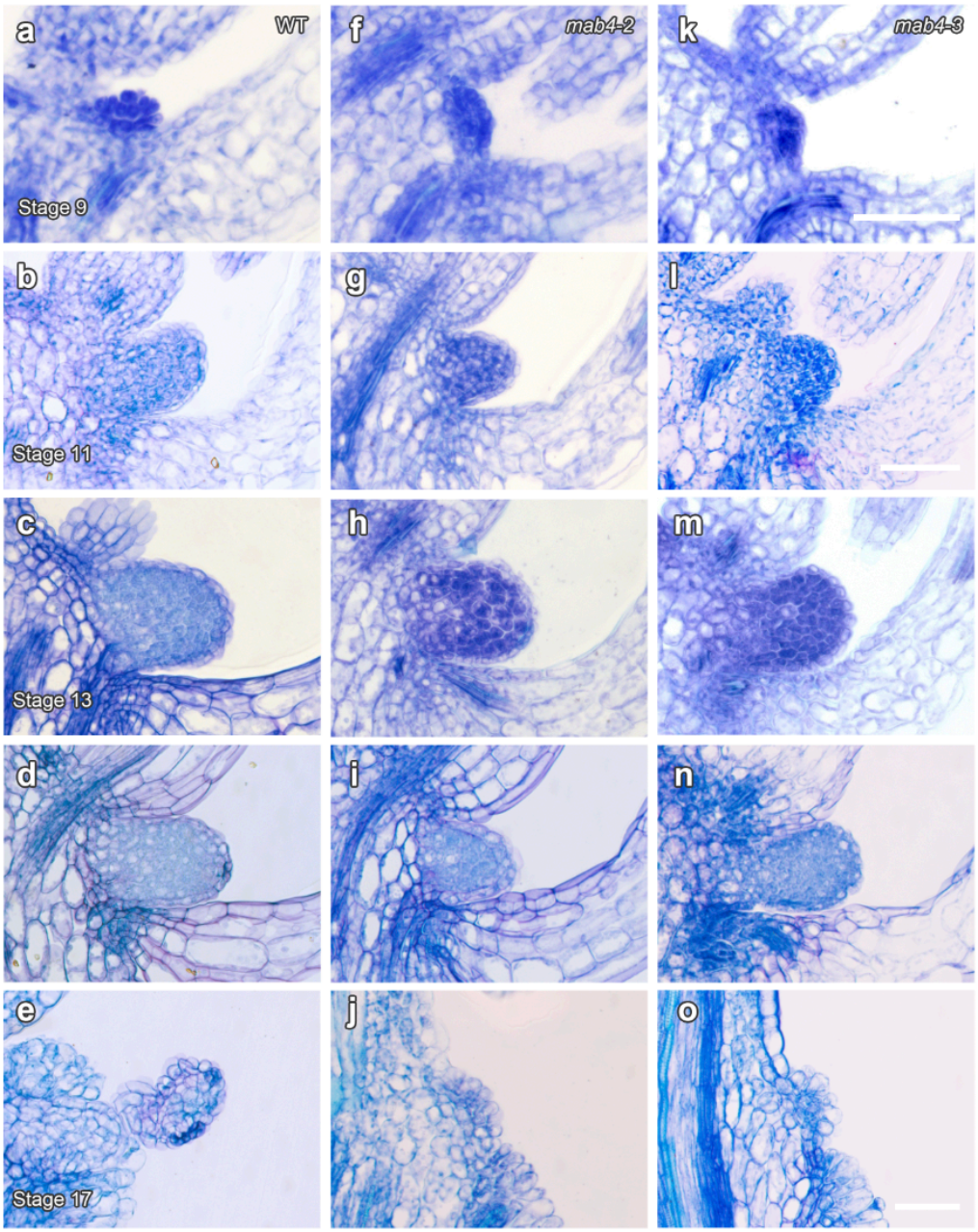

Supplementary Fig. 17 Internal structure of a nectary in the flowers of *mab4* mutants.

a–e, Longitudinal sections of nectaries from WT (Col-0) flowers at stage 9 (**a**), stage 11 (**b**), stage 13 (**c**), stage 15 (**d**) and stage 17 (**e**). **f–j**, Longitudinal sections of nectaries from *mab4-2* flowers at stage 9 (**f**), stage 11 (**g**), stage 13 (**h**), stage 15 (**i**) and stage 17 (**j**). **k–o**, Longitudinal sections of nectaries from *mab4-3* flowers at stage 9 (k), stage 11 (**l**), stage 13 (**m**), stage 15 (**n**) and stage 17 (**o**). Scale bars, 50 μm.

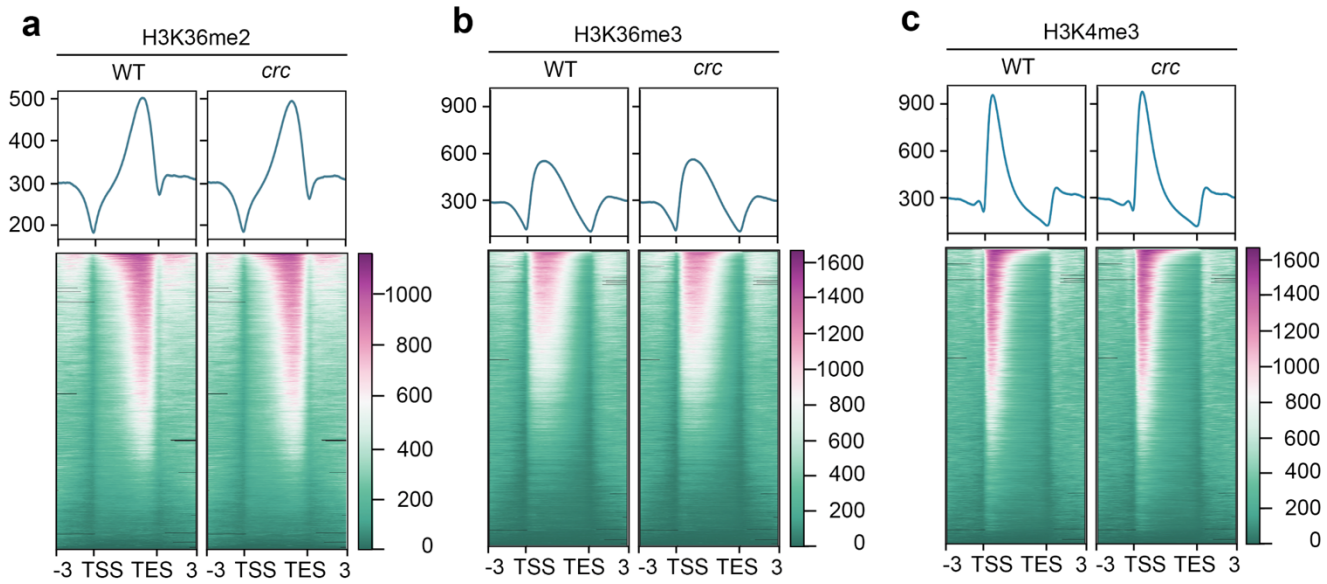

Supplementary Fig. 18 Histone modifications in wild type and *crc*.
a–c, Averaged profiles of ChIP-seq signal intensity around genes in wild type (left) and the *crc-1* mutant (right). ChIP-seq results for histone H3K36me2 (**a**), H3K36me3 (**b**) and H3K4me3 (**c**).

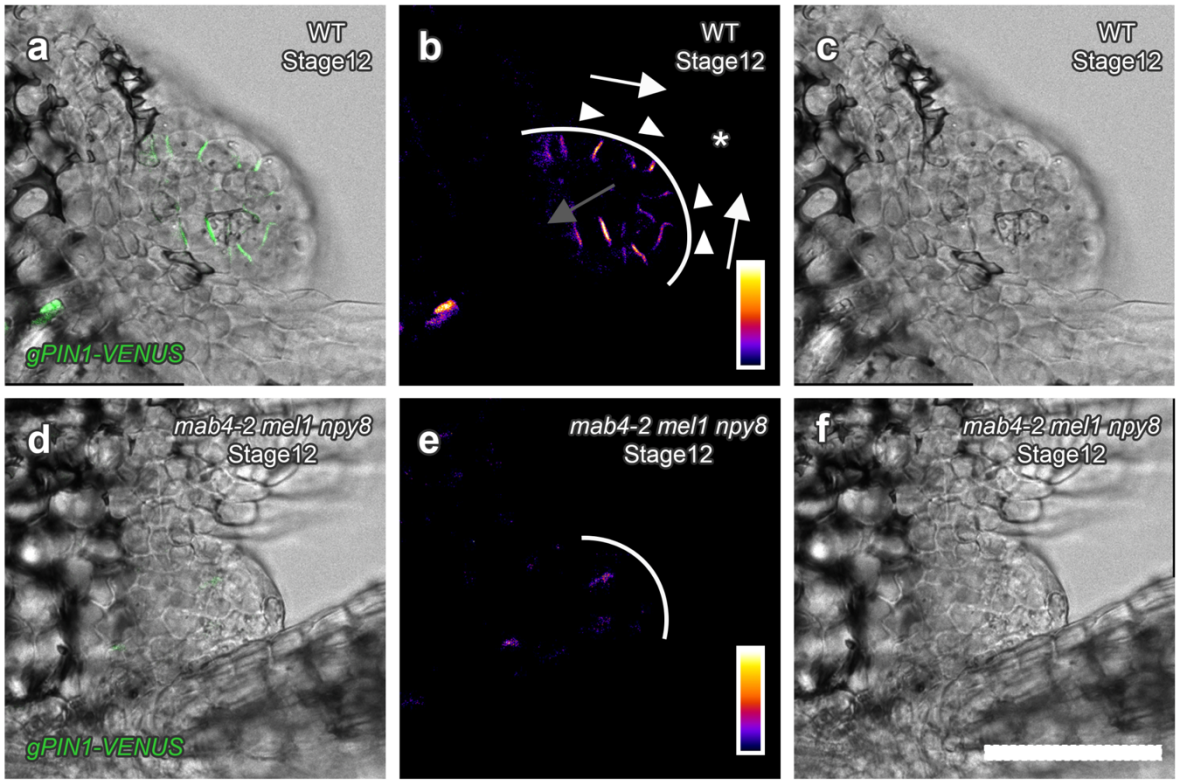

Supplementary Fig. 19 gPIN1-VENUS accumulation in the *mab4 mel1 npy8* triple mutant.

a–f, gPIN1-VENUS accumulation in longitudinal sections of nectaries from WT (**a–c**) and *mab4-2 mel1 npy8* (**d–f**) flowers at stage 12. Longitudinal sections of merged images (**a, d**), GFP fluorescence images with Fire LUT applied in image J (**b, e**) and bright-field images (**c, f**) are shown. Nectary outlines are indicated by white lines. Scale bar, 50 μm.

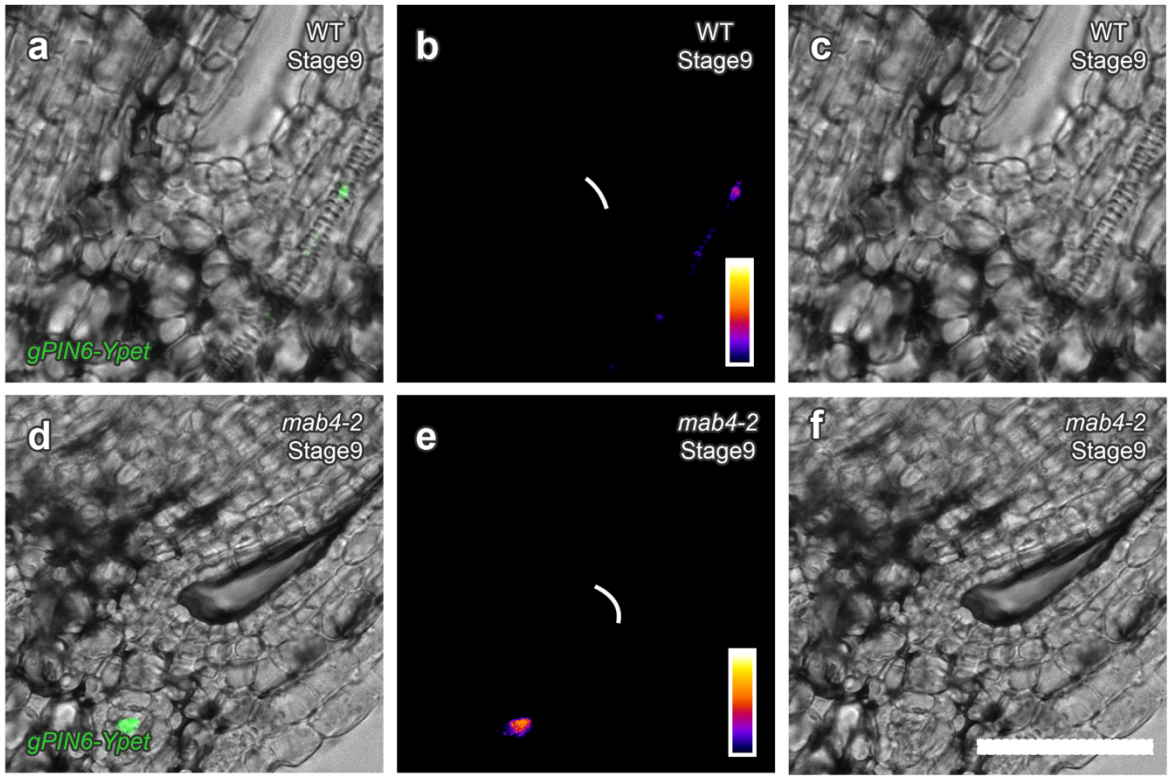

Supplementary Fig. 20 gPIN6-Ypet accumulation in the *mab4-2* mutant. **a–f**, gPIN1-Ypet accumulation in longitudinal sections of nectaries from WT (L*er*) (**a–c**) and *mab4-2* (**d–f**) flowers at stage 9. Longitudinal sections of merged images (**a, d**), GFP fluorescence images with Fire LUT applied in image J (**b, e**) and bright-field images (**c, f**) are shown. Nectary outlines are indicated by white lines. Scale bar, 50 µm.

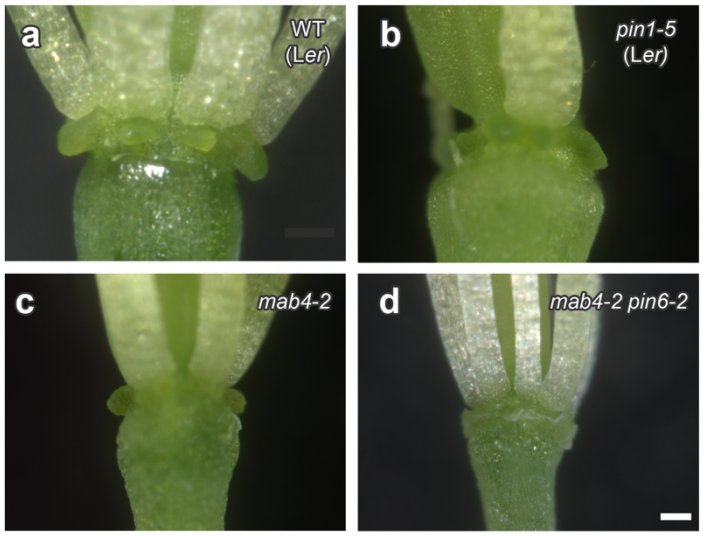

Supplementary Fig. 21 Close-up views of nectaries from the flowers of various mutants.
a–d, Side views of nectaries from stage 13 flowers of WT (L*er*) (**a**), *pin1-5* (**b**), *mab4-2* (**c**) and *mab4-2 pin6-2* (**d**). Scale bar, 100 μm.